

Mesoscale Predictability of the “Surprise” Snowstorm of 24–25 January 2000

F. ZHANG

National Center for Atmospheric Research, Boulder, Colorado, and
Department of Atmospheric Sciences, Texas A&M University, College Station, Texas*

CHRIS SNYDER AND RICHARD ROTUNNO

National Center for Atmospheric Research, Boulder, Colorado

(Manuscript received 24 May 2001, in final form 11 December 2001)

ABSTRACT

A mesoscale model is used here to investigate the possible sources of forecast error for the 24–25 January 2000 snowstorm along the east coast of the United States. The primary focus is the quantitative precipitation forecast out to lead times of 36 h. The success of the present high-resolution control forecast shows that the storm could have been well forecasted with conventional data in real time. Various experiments suggest that insufficient model grid resolution and errors in the initial conditions both contributed significantly to problems in the forecast. Other experiments, motivated by the possibility that the forecast errors arose from the operational analysis poorly fitting one or two key soundings, test the effects of withholding single soundings from the control initial conditions. While no single sounding results in forecast changes that are more than a small fraction of the error in the operational forecast, these experiments do reveal that the detailed mesoscale distribution of precipitation in the 24- or 36-h forecast can be significantly altered even by such small changes in the initial conditions. The experiments also reveal that the forecast changes arise from the rapid growth of error at scales below 500 km in association with moist processes. The results presented emphasize the difficulty of forecasting precipitation relative to, say, surface pressure and suggest that the predictability of mesoscale precipitation features in cases of the type studied here may be limited to less than 2–3 days.

1. Introduction

On 24–25 January 2000, an intense winter storm off the southeastern coast of the United States brought heavy snowfalls from the Carolinas through the Washington, D.C., area and into New England. Snow fell across North Carolina with the Raleigh–Durham area reporting a record snowfall total from the storm of over 20 in. [according to the records provided by National Climate Data Center (NCDC) dating back to 1887]. Although the errors in position and intensity of the surface cyclone were not exceptional, the precipitation forecast by the operational models running at the National Centers for Environmental Prediction (NCEP) posed a serious challenge for forecasters in the affected region. Figure 1 shows the 24-h observed accumulated precipitation in liquid water content between 1200

UTC 24 and 1200 UTC 25 January 2000, the corresponding operational Eta Model forecast, and the research-model forecast (both models were initialized at 0000 UTC 24 January 2000). Except for some light precipitation on the coast of North Carolina, the operational Eta Model (32-km resolution) missed most of the precipitation over land all along the Atlantic coast (Fig. 1b) while our research model (details discussed later) produced an excellent 24-h accumulated precipitation forecast (Fig. 1c). The purpose of this study is to explore through sensitivity experiments the possible reasons for the success of the research-model forecast. The results of these experiments are of interest for what they reveal both about the specific storm and about the limits of predictability of precipitation within winter storms.

The notion of a limit of predictability originated with Lorenz (1969), who suggested that skillful weather forecasts would be limited to a finite lead time even for forecast models and initial conditions of much greater accuracy than are presently available. This limit of predictability, which depends upon the scale of interest, is thought to be on the order of 2 weeks (see, for example, section 4 of Simmons et al. 1995) for total wavenumbers less than about 40 on the sphere. On the mesoscale

* The National Center for Atmospheric Research is sponsored by the National Science Foundation.

Corresponding author address: Dr. Fuqing Zhang, Department of Atmospheric Sciences, Texas A&M University, 3150 TAMU, College Station, Texas 77843-3150.
E-mail: fzhang@tamu.edu

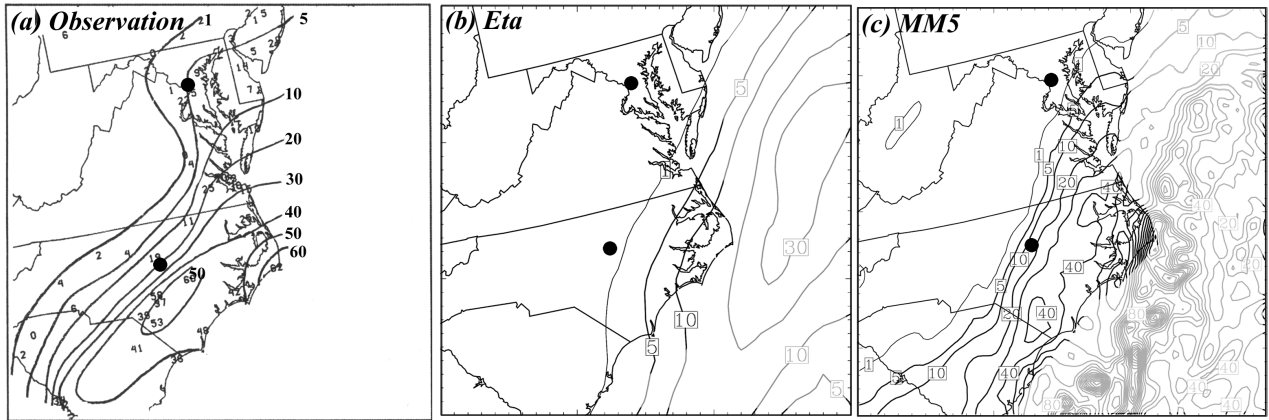


FIG. 1. The 24-h accumulated precipitation (mm) in liquid water content from 1200 UTC 24 to 1200 UTC 25 Jan 2000. (a) Subjective observational analysis, (b) the operational Eta Model forecast, and (c) the MM5 Cntl-3.3km forecast. Both models initialized at 0000 UTC 24 Jan 2000. The precipitation forecast over the ocean is contoured in gray lines.

(where most of the interesting structure in precipitation lies), it remains an open question whether the predictability limit is a few 10s of hours or several days. The initial results of Anthes et al. (1985) indicated that the mesoscale enjoyed enhanced predictability but their results were subsequently found to arise from the perfectly known lateral boundary conditions they employed (Vukicevic and Errico 1990). More recent work (Ehrendorfer et al. 1999) has revealed that initial errors can grow rapidly in limited-area models, yet the mechanisms that control the growth of forecast errors and the loss of predictability are still poorly understood. The simulations of the January 2000 snowstorm discussed below provide concrete examples of such mechanisms and serve as an initial step in quantifying and understanding mesoscale predictability, particularly of precipitation.

The approach utilized here simulates the storm with the Pennsylvania State University–National Center for Atmospheric Research (PSU–NCAR) nonhydrostatic fifth-generation Mesoscale Model (MM5) version 2 (Dudhia 1993), using the real-time Eta forecasts for the lateral boundary conditions, so that the MM5 simulations are equivalent to real-time forecasts. Then, it is asked how various model configurations and/or initial conditions contribute to the skill of this simulation. Lacking knowledge of systematic biases between MM5, Eta, or any other mesoscale models, the approach here is to use MM5 as a vehicle to discover the generic sources of forecast error in this case (and by extension, similar cases). Several previous studies have considered forecasts of specific winter storms. Orlanski and Katzfey (1987) used a nested global, limited-area model to predict the Presidents’ Day cyclone of 18–19 February 1979. They found that the most important improvement in storm forecast came from increased horizontal resolution, consistent with previous studies by Anthes et al. (1983) and Kocin et al. (1985). They also found the increasing importance of the lateral boundary conditions with time in the limited-area forecast. In the numerical

investigation of a rapid mesoscale cyclogenesis that occurred on 28–29 March 1984, Kuo et al. (1995) concluded that because of the diabatic nature of the weather system, the forecast was highly sensitive to initial condition and thus imposed a limit on mesoscale predictability. The “superstorm” of March 1993 was one of the most successful long-range heavy snow and blizzard forecasts ever for a major winter storm, however, predictions of important mesoscale elements of the storm were still problematic (Uccellini et al. 1995; Hou et al. 1995). With the dramatic advancement of computational capability during the past decade, regional/mesoscale models will shortly have resolution close to that needed to resolve convection explicitly, hence researchers are now in a position to reassess the roles of model resolution and initial conditions in severe winter-storm predictions.

The present study focuses on the precipitation forecast at relatively short range (0–36 h) and relatively high resolution (down to 3.3 km), and on its sensitivity with respect to model grid resolution (in section 5) and the initial state (in section 6). As found in previous studies, significant improvements of the MM5 forecasts can be achieved with finer grid resolution. The importance of the initial conditions is investigated by initializing MM5 with different analyses, including those from various operational centers, and the standard MM5 initialization in which existing surface and upper-air observations are reanalyzed with a Cressman-type objective analysis scheme (Benjamin and Seaman 1985) using the operational-Eta analysis as a first guess. Such changes in the initial conditions can alter this simulation by an amount comparable to the error in the operational forecasts, which is to be expected given the sensitivity of midlatitude forecasts to initial conditions demonstrated, for example, by Rabier et al. (1995). As will be shown in section 6, however, the changes in this study’s simulations arise not, as in Rabier et al. (1995), through the growth of forecast differences at the synoptic scale,

but through rapid growth in the presence of moisture of differences at meso- and smaller scales.

These experiments lead naturally to further questions concerning the mechanisms for and characteristics of the error growth as well as the ultimate predictability of precipitation at these scales, which will be addressed in a companion paper. A brief overview of the storm is presented in section 2. The model and experimental design are described in section 3. Section 4 compares the control simulation with observations. Sensitivity tests with respect to model grid resolution are reported in section 5. The sensitivity to initial state and lateral boundary conditions is analyzed in section 6. Section 7 contains the summary and discussions.

2. Overview of the storm

The storm began as an upper-level short wave embedded in a broad synoptic trough over the eastern United States and then moved southward, across the southeastern states. A 300-hPa low center formed near the coast of Georgia and South Carolina by 0000 UTC 25 January 2000 (Fig. 2a). This low center moved north, along the Atlantic Coast, reaching southeastern North Carolina by 1200 UTC 25 January (Fig. 2b) and the Washington, D.C., area by 1800 UTC 25 January 2000. Figure 3 shows the surface observational analysis and column maximum radar reflectivity at 0000 and 1200 UTC 25 January 2000, during which period Raleigh, North Carolina, had the most intense snowfall. Surface observations of the minimum mean sea level pressure associated with the cyclone showed a rapid drop of 22 hPa in 24 h, from 1005 hPa at 1200 UTC 24 January (not shown) to 983 hPa at 1200 UTC 25 January (Fig. 3b). The low deepened rapidly and followed the upper-level system (Fig. 2), moving almost northward just off the North Carolina coast and reaching the coast of Maryland by 1800 UTC January. Continuing on a more north-northeast path, the storm reached New England on 26 January 2000.

3. Model description and experimental design

The two-way nested PSU–NCAR nonhydrostatic Mesoscale Model MM5, version 2 was used for this study (Dudhia 1993). The control simulation shown in Fig. 1c (hereafter also referred to as Cntl-3.3km) was initialized at 0000 UTC 24 January 2000 with operational Eta Model 104-grid (~ 85 km horizontal resolution) data reanalyzed with conventional observations, employing three model domains (D1, D2, D3) with 30, 10, and 3.3 km grid resolution, respectively. The 30-km coarse domain employs 120×190 grid points with 27 vertical layers, covering the entire continental United States, while the number of grid points for both the 10- and 3.3-km nested domains are 181×241 . The finest-resolution 3.3-km domain is movable and adjusted every 3 h following the strongest precipitation. The model

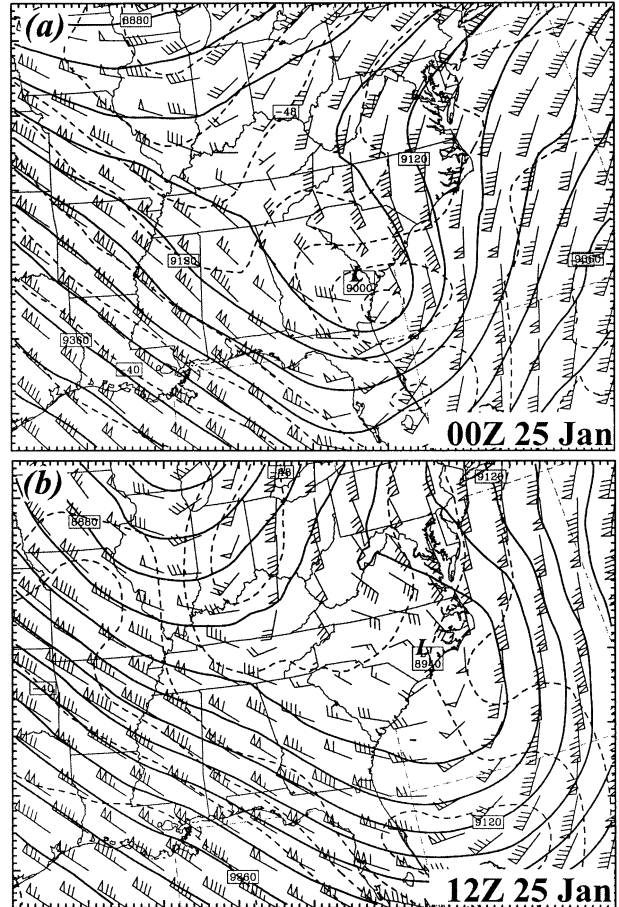


FIG. 2. MM5 observational analysis of 300-hPa winds (full barb denotes 5 m s^{-1}), geopotential heights (solid, every 6 dam), and temperature (dashed, every 2 K) valid at (a) 0000 and (b) 1200 UTC 25 Jan 2000.

domains are shown in Fig. 4 (the location of D3 at 0000 UTC 25 January 2000 is shown). The Mellor–Yamada PBL scheme (Mellor and Yamada 1982) and Reisener microphysics scheme with graupel (Reisener et al. 1998) are used for all three domains. Domains D1 and D2 use the Grell cumulus parameterization scheme (Grell 1993) while D3 is fully explicit. The simulation used the operational Eta Model 104-grid forecasts for the lateral boundary conditions updated every 6 h, so that this simulation is equivalent to a real-time forecast.

Two experiments have been performed to test the forecast sensitivity to model grid resolutions: “Cntl-10km” is as in Cntl-3.3km, but without D3; “Cntl-30km” has only D1.

A series of experiments has been designed to test the sensitivity of the storm prediction to model initial states. First, the experiments “EtaOnly” and “EcmOnly” are used to study the impacts of different data sources on the MM5 initialization; EtaOnly is identical to Cntl-30km except that the conventional

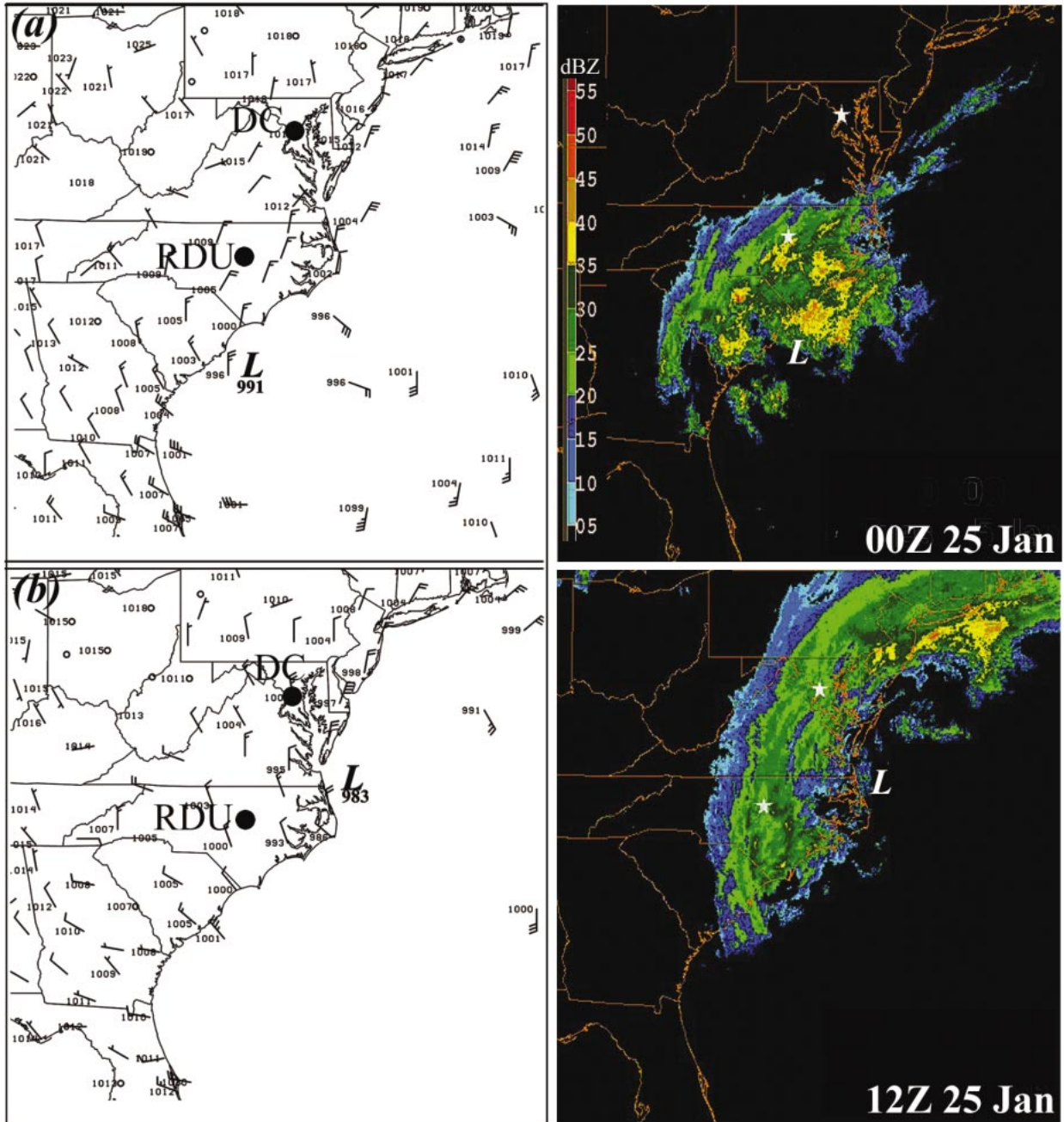


FIG. 3. Observations of surface winds (full barb denotes 5 m s^{-1}), MSLP (left), and observed column max radar reflectivity (right) valid at (a) 0000 and (b) 1200 UTC 25 Jan 2000. Here, DC and RDU denote Washington, DC, and Raleigh, NC, respectively.

observations are not reanalyzed by the MM5 preprocessor programs in this simulation, and thus the initial conditions are simply the Eta analysis interpolated to the MM5 grid; EcmOnly is similar to EtaOnly except that the analysis from European Centre for Medium-Range Weather Forecasts (ECMWF) has been used for the initialization and boundary conditions, instead of the operational Eta analysis and forecasts. The ECMWF analyses are archived at NCAR on a $128 \times$

64, global, Gaussian grid and subsequently interpolated to the MM5 grid.

Various experiments have been performed to test the effects of individual soundings on the storm prediction. Experiments have also been designed to study model sensitivity to the above factors in the “fake-dry” environment by turning off the latent heating-cooling feedback. These experimental designs will be discussed in the following sections.

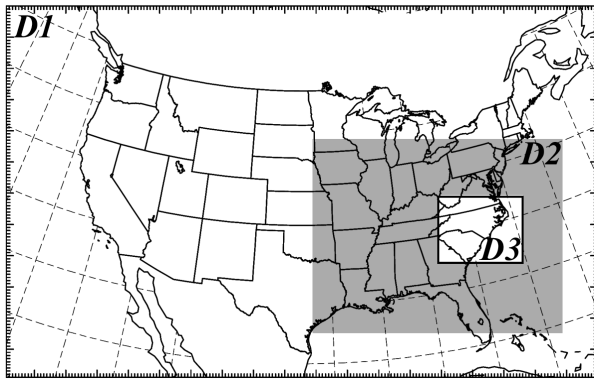


FIG. 4. The relative locations of MM5 model domains. The grid resolutions of D1, D2, and D3 are 30, 10, and 3.3 km, respectively. Here, D3 is moveable with the snapshot location valid at 0000 UTC 25 Jan 2000.

4. Control simulation

Figures 5a and 5b show the MM5 Cntl-3.3km forecast for mean sea level pressure (MSLP), surface winds, and low-level averaged radar reflectivity valid (on D3, see Fig. 4) at 0000 and 1200 UTC 25 January 2000. Figures 5a and 5b can be compared to Figs. 3a and 3b, which show the corresponding observed MSLP and surface winds together with column maximum radar reflectivity. The location and central pressure of the cyclone from the Eta analysis are shown in Fig. 3. The 24-h and 36-h MM5 forecast has captured the location and strength of the rapidly developing cyclone as well as the precipitating cloud over the Carolinas, though the 36-h forecast has the cloud band too far east. Figure 6 shows the control forecast and the observed 6-h accumulated precipitation (in liquid water content) between 0000 and 0600 UTC 25 January, during which period Raleigh, North Carolina, had the most intense snowfall. The control precipitation forecast (Figs. 1c, 6a) compares reasonably well with the observations (Figs. 1a, 6b). The upper-level short-wave trough associated with the potential vorticity anomaly as well as the jet structure and strength (not shown) are also well simulated by the model. Analysis also shows that the model well handles both the evolution of precipitation type and the location of the surface freezing line (not shown). However, the model forecast is far from perfect. The simulated precipitation boundary still lies ~ 50 – 100 km to the east and southeast of the observed boundary, and the heaviest precipitation is slightly underestimated.

In summary, the control run shows that the rapid cyclogenesis and attendant precipitation features in this case can be forecast relatively accurately by mesoscale models with conventional data. Other examples of reliable mesoscale forecasts from conventional data can be found in Kocin et al. (1985) and Zhang et al. (2001). The following section will look into various factors that contribute to the sensitivity of this record-breaking snowfall forecast.

5. Sensitivity to grid resolution

Two experiments have been performed to study the forecast sensitivity to model grid resolution. Cntl-10km is as in Cntl-3.3km but without the 3.3-km grid domain, while Cntl-30km has only the 30-km coarse domain. These simulations show that the forecast quality will be systematically degraded when going to coarser horizontal grid resolutions for this case. Figures 5c and 5d show both Cntl-10km and Cntl-30km simulated MSLP, surface winds, and model-derived low-level averaged radar reflectivity at 0000 UTC 25 January 2000 (24-h forecasts) over the same domain as in Fig. 3a. From the comparison of Figs. 5a, 5c, and 5d, as will be discussed below, refining resolution from 30 km to 10 km provides most of the benefit, while the improvement from 10 km to 3.3 km is relatively small. This is rather encouraging since present computational resources allow 10-km operational forecasts at least regionally, while the forecast with 3.3-km resolution remains impractical in real time.

Figures 7a and 7b show the Cntl-30km 6-h and 24-h accumulated precipitation forecasts, which may be compared against those from the Cntl-3.3km simulation shown in Fig. 6a and Fig. 1c, respectively. Though the Cntl-30km run produced cyclogenesis accurately off the Carolina coast, the precipitation band over land is less organized and further to the east (Figs. 5d, 7).

In this event nearly all precipitation over land throughout the 48-h simulation is produced by explicit microphysics, rather than by the cumulus parameterization scheme, even in the Cntl-30km (30-km domain only) run. The higher-grid-resolution (10- and 3.3-km) simulations have the apparent advantage of representing the grid-scale precipitation more realistically than the 30-km run. Considerably stronger and more accurate precipitation has been simulated over Louisiana, Georgia, and later in the Carolinas in Cntl-3.3km than in Cntl-30km.

It is natural to ask why resolution helps. Obvious candidates are the improved representation of moist processes (e.g., Davis et al. 1993; Kuo et al. 1991; Bosart et al. 1995; Dickinson et al. 1997), since it is well known that they are crucial to such rapidly deepening cyclones and that they tend to enhance scale contraction of frontal structures (Emanuel 1985; Whitaker and Davis 1994). The feedback by latent-heat release is also essential in the explosive cyclogenesis as demonstrated by the following fake-dry simulations. Two fake-dry simulations, "FD-10km" and "FD-30km," have been set up and run exactly the same as in Cntl-10km and Cntl-30km, respectively, except that the latent-heat release has been turned off in both simulations. Figure 8 shows the mean sea level pressure forecasts from the two fake-dry simulations. Though there is still cyclogenesis in the fake-dry simulations, both FD-10km and FD-30km produce much weaker surface lows. Also, there is no enhancement of the surface cyclone with improved resolution in these fake-dry simulations, further suggesting that

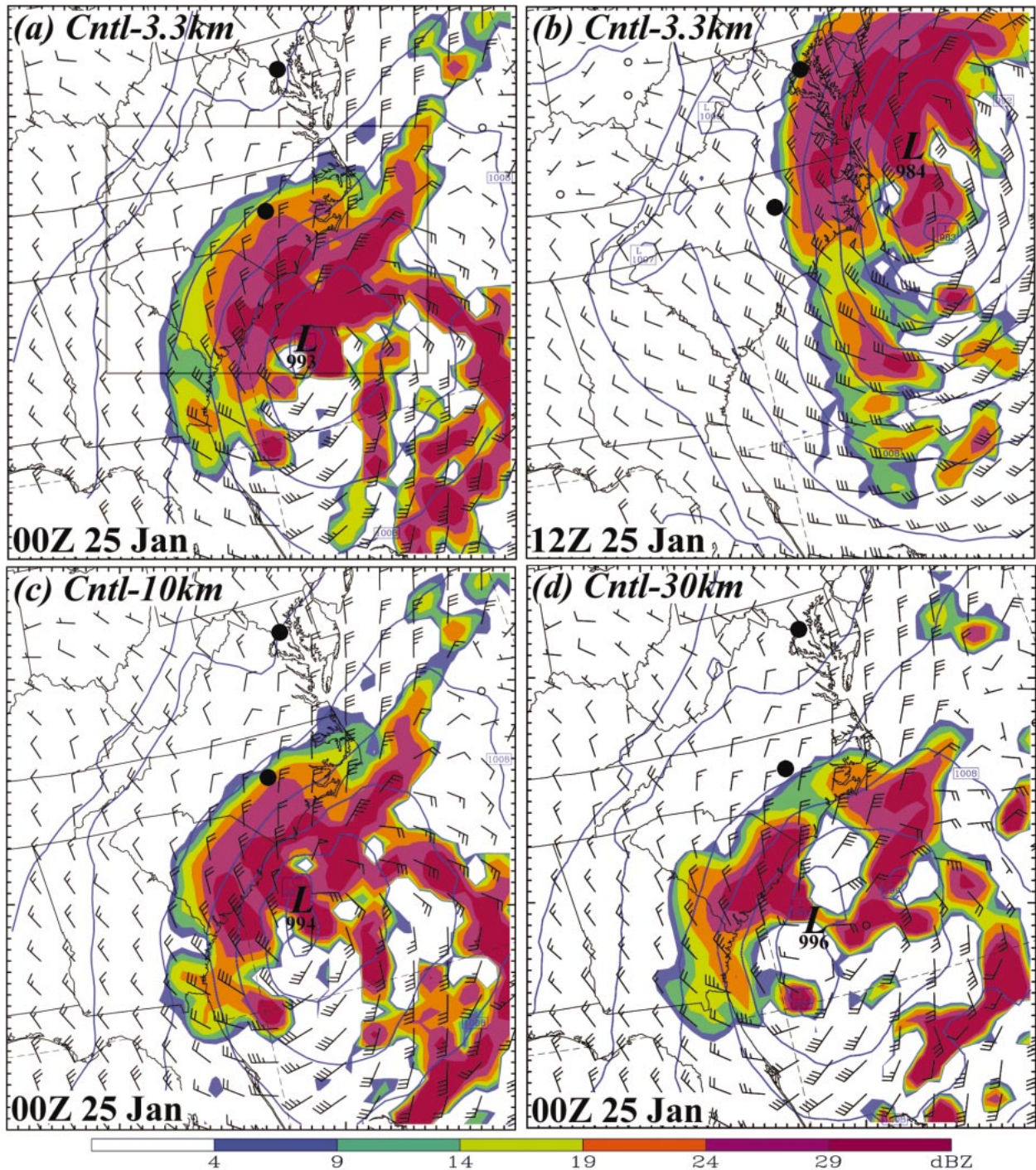


FIG. 5. (a)–(b) Cntl-3.3km forecast MSLP (every 4 hPa), lowest sigma-level winds (full barb denotes 5 m s^{-1}) and model derived low-level (sigma greater than 0.710) averaged reflectivity (dBZ) valid at (a) 0000 and (b) 1200 UTC 25 Jan 2000. The location of D3 at 0000 UTC 25 January is framed in (a). (c)–(d) As in (a) except for (c) Cntl-10km and (d) Cntl-30km.

the benefits of increased resolution in the control simulations come from better representation of the moist processes.

In this particular case, there is evidence that better resolution of moist processes results in crucial changes

to the simulation of upper-level features. Figure 9 shows the comparison of the 300 hPa potential vorticity (PV), geopotential height, and winds at 0000 UTC 25 January from Cntl-3.3km (Fig. 9a) and Cntl-30km (Fig. 9b) from the same 30-km grid domain as well as the difference

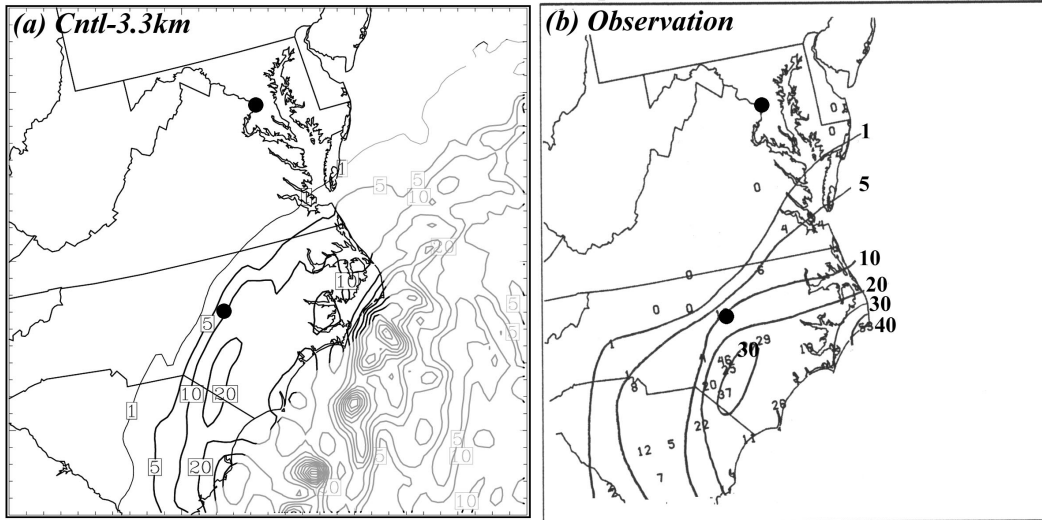


FIG. 6. The 6-h accumulated precipitation (mm) in liquid water content from 0000 to 0600 UTC 25 Jan 2000. (a) Cntl-3.3 km forecast, and (b) subjective observational analysis.

of their PV and wind vectors (Fig. 9c). There are several noticeable differences between these two simulations at this level. With better-resolved moist processes and stronger diabatic heating in Cntl-3.3km, a stronger negative PV anomaly builds directly above the precipitating system (Fig. 9c). This finding is consistent with that of Davis et al. (1993), where latent heating is identified as a main contributor to the upper-level anticyclone (see their Figs. 7 and 9). As a result, there is a considerably stronger anticyclonic flow along the Atlantic coast. This stronger upper-level coastal ridge implies more north-westward winds in the Carolinas, which in turn drive the precipitation band more to the northwest and on-shore, as apparently occurred in the real event (Fig. 3a).

6. Sensitivity to initial state

As discussed in the previous section, increased model grid resolution significantly improved the model forecast. However, the coarse-resolution experiment (Cntl-30km), with resolution comparable to the operational Eta Model (32-km resolution), still improved on the operational forecast, suggesting factors other than grid resolution contributed to the forecast sensitivity. In this section, there will be investigation of how reasonable changes to the initial conditions alter the MM5 forecast.

a. Initial data sources

First, there is consideration of how the forecasts might be altered by using analyses from different operational centers as initial conditions. For the EtaOnly experiment, MM5 is initialized with the Eta analysis at 0000 UTC 24 January 2000 but without reanalyzing observations as was done in Cntl-30km, that is, the initial analysis from the operational Eta Model 104-grid (~85

km grid resolution) is directly interpolated onto the MM5 grids. Similarly, for the EcmOnly experiment, MM5 is initialized at 0000 UTC 24 January 2000 by interpolating the ECMWF global analysis (archived at NCAR on a $2.5^\circ \times 2.5^\circ$ grid) to the MM5 grid. The archived forms of both the Eta and the ECMWF analyses used to initialize MM5, therefore, have reduced resolution compared to the operational analyses. The resolutions of the operational Eta and ECMWF analyses were 32 km and ~65 km at the time of the storm.

Figure 10 shows the 300-hPa initial magnitude of wind speed differences between Cntl-30km and EtaOnly and between Cntl-30km and EcmOnly. There are significant initial upper-level wind differences between Cntl-30km and EtaOnly. For example, the wind in Cntl-30km at Little Rock, Arkansas (LZK), differs from the Eta analysis at 0000 UTC 24 January by 12.2 m s^{-1} ; differences of $5\text{--}10 \text{ m s}^{-1}$ along the jet core can be found in several other sounding locations. Even greater differences exist between Cntl-30km and EcmOnly, such as the 16.7 m s^{-1} wind difference at LZK (Fig. 10b).

At 30 h (Figs. 11a–c), forecasts from these alternative initial conditions exhibit substantial differences in precipitation from Cntl-30km, and less marked, but still significant, differences in surface pressure. In EtaOnly (Fig. 11b), the onshore precipitation over the Carolinas is weaker (indeed, all but absent in South Carolina) and shifted further east, with most of the precipitation falling as rain or mixed rain (not shown). The strength and positioning of the simulated cyclone center, however, are similar to those of the Cntl-30km but with slightly higher pressure along the coast of the Carolinas and a 120-km shift of cyclone center. If the ECMWF global analysis is used to initialize MM5, differences are larger, consistent with the larger differences in the initial con-

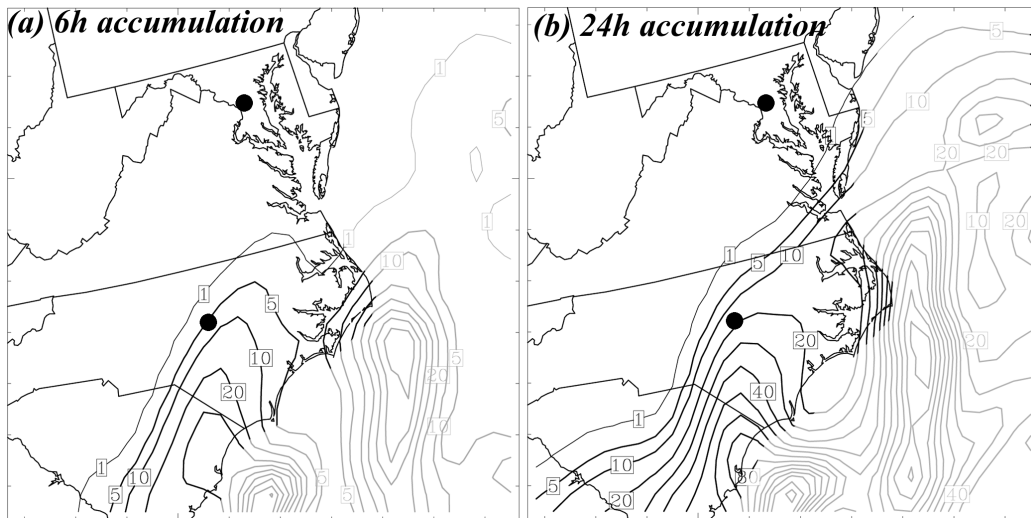


FIG. 7. (a) As in Fig. 6(a) except for Cntl-30km. (b) As in Fig. 1(c) except for Cntl-30km.

ditions (Fig. 10b), and virtually all the precipitation occurs offshore during the period of most intense snowfall at Raleigh (Fig. 11c). The forecast of mean sea level pressure in EcmOnly is also noticeably degraded, though it captures the general synoptic pattern, with low pressure off the North Carolina coast. The differences in the precipitation between either simulation and Cntl-30km are even greater for 24-h accumulations ending at 36 h (compare Figs. 12a,b with Fig. 7b).

Thus, the storm forecast is sensitive to changes of the initial conditions that are within the uncertainty of the operational analyses. To the extent that small-scale motions influence precipitation more than mean sea level pressure, the relatively large precipitation differences seen in Fig. 11 (as compared to differences in sea level

pressure) also suggest that forecast divergence between these two simulations is concentrated at smaller scales.

Spectral analysis of the difference kinetic energy is now used to quantify the forecast divergence at different scales. Difference kinetic energy (DKE) per unit mass is defined as:

$$DKE = 1/2 \sum (U'_{ijk}{}^2 + V'_{ijk}{}^2), \quad (1)$$

where U' and V' are the difference wind components between two simulations and i, j, k run over x, y , and σ grid points.

Figure 13a shows the spectrum analysis of DKE for the difference between Cntl-30km and EtaOnly at the 0- and 36-h forecast times. The inference that the forecasts diverge at the smaller scales is correct: the forecast

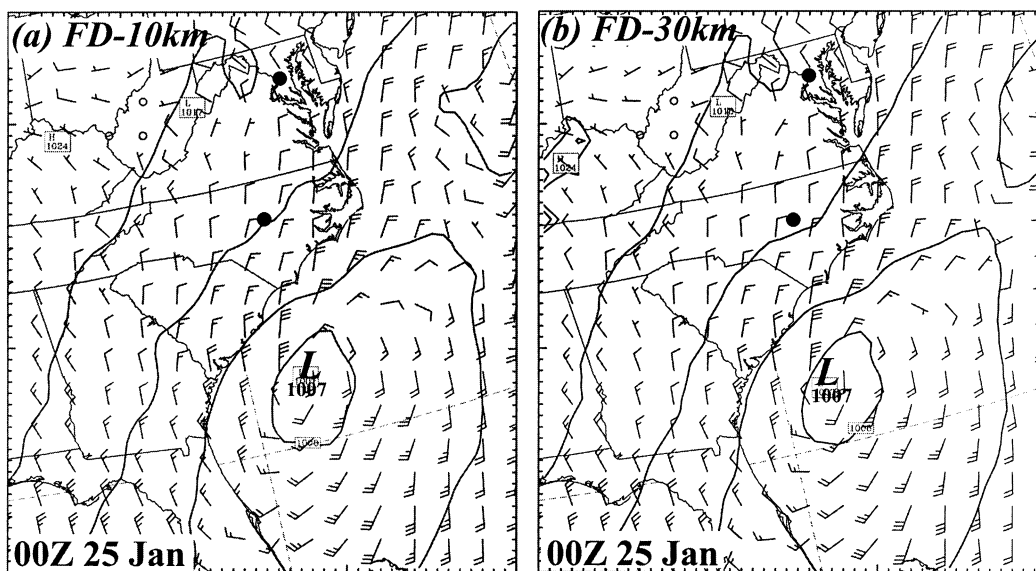


FIG. 8. As in Fig. 5(a) except for (a) FD-10km and (b) FD-30km.

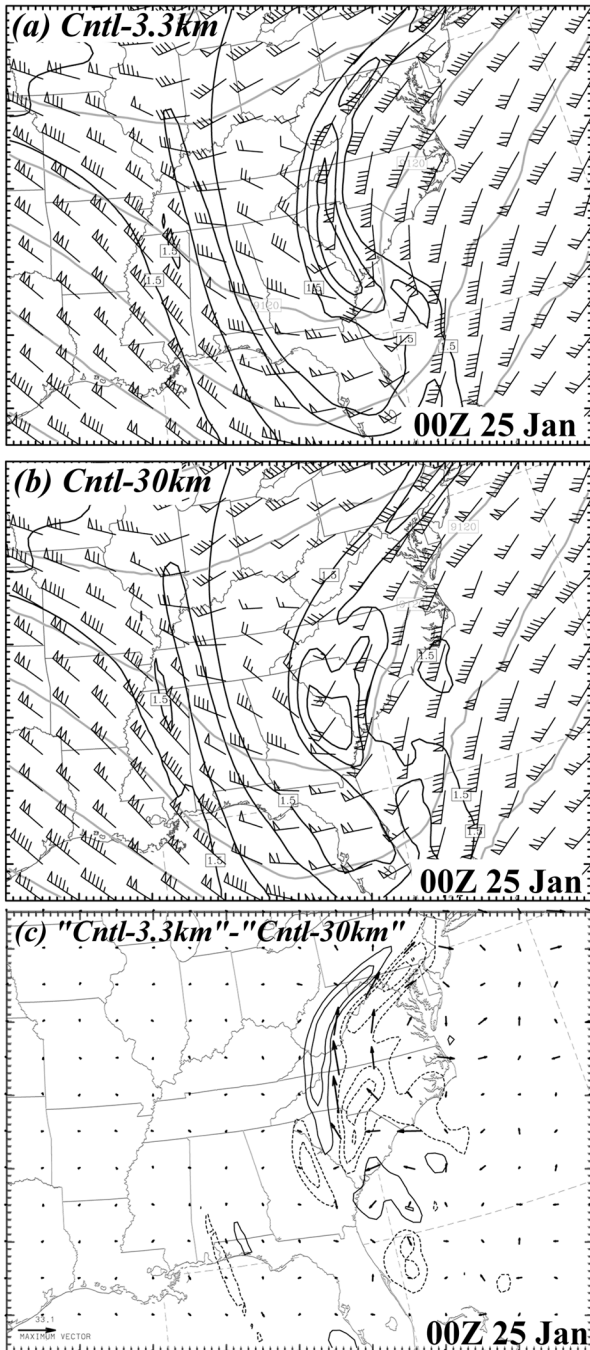


FIG. 9. MM5 simulated 300-hPa winds, geopotential heights (gray, every 12 dam), and PV (solid, every 1.5 PVU) at 0000 UTC 25 Jan 2000 for (a) Cntl-3.3km and (b) Cntl-30km. (c) Difference winds and PV (every 1.0 PVU).

difference decays significantly at wavelengths greater than 900 km but grows rapidly at wavelengths below 600 km. The wavelength bands of decay and growth correspond broadly to the synoptic scale and to meso- and smaller scales, respectively. For brevity, hereafter reference to these bands will often be simply larger and

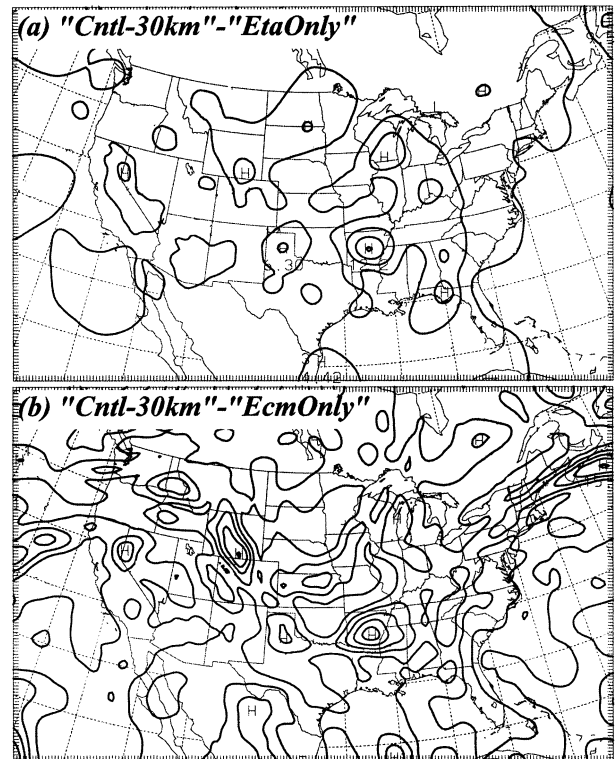


FIG. 10. The 300-hPa magnitude of wind difference (every 3 m s⁻¹) valid at 0000 UTC 24 Jan 2000 between Cntl-30km and (a) EtaOnly, (b) EcmOnly.

smaller scales. The reasons for both the growth at smaller scales and the decay at larger scales are discussed further in section 6c.

b. Sensitivity to individual soundings

The initial conditions in EtaOnly differed significantly from the rawinsonde observations in a few locations (Fig. 10). With the reanalysis of the sounding observations, the initial conditions in Cntl-30km fit the observations much better. Thus, it seems possible that one (or a few) sounding(s) might have been crucial to the improved forecast of Cntl-30km relative to that from EtaOnly, and also to the operational-forecast failure.

Figure 10a shows that the biggest difference in the initial analyses between the Cntl-30km and EtaOnly was at LZK. Hence to test the effect of this sounding on the forecast, a numerical forecast was conducted in which the initial analysis was done by exactly the same procedure as in Cntl-30km, except that the LZK sounding observation was omitted in the MM5 reanalysis (this forecast is called NoLZK). Comparison of Fig. 11d (NoLZK) with Fig. 11a (Cntl-30km) shows that the NoLZK forecast is markedly more similar to Cntl-30km than it was to EtaOnly (Fig. 11b). Thus, it does not appear that omission of the LZK sounding can account for the differences between Cntl-30km (Fig. 11a) and EtaOnly (Fig. 11b).

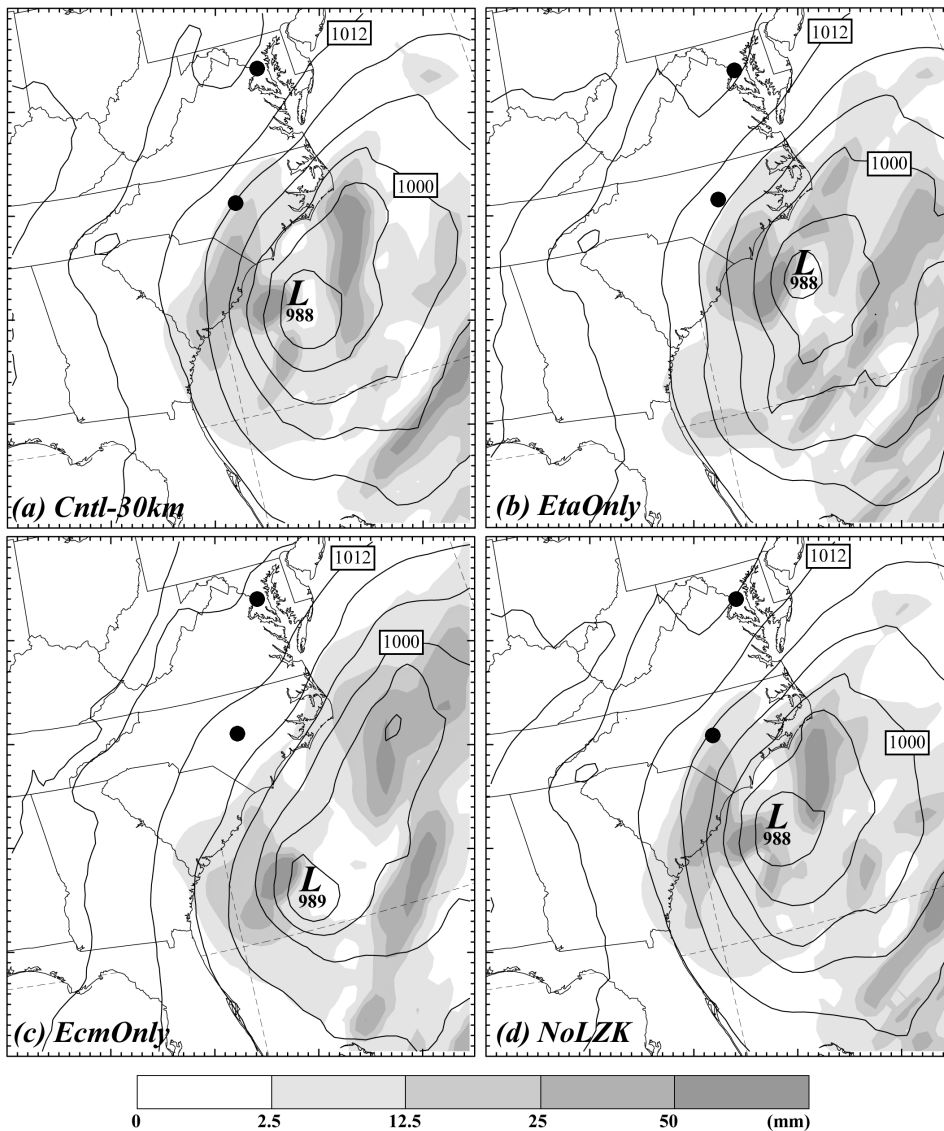


FIG. 11. MM5 simulated MSLP (solid lines, every 4 hPa) and 6-h accumulated precipitation (mm, shaded) valid at 0600 UTC 25 Jan 2000 for (a) Cntl-30km, (b) EtaOnly, (c) EcmOnly, and (d) NoLZK.

Although the surface pressure forecasts are nearly identical, the NoLZK forecast (Fig. 11d) does have noticeable differences with the Cntl-30km forecast (Fig. 11a) with respect to the 6-h accumulated precipitation, suggesting similarity in the larger-scale pattern with more noticeable differences in the embedded small-scale structures. Another view of the scale dependence of the forecast difference is contained in Fig. 14a, which shows the magnitude of the 300-hPa initial wind difference (in gray contours) between Cntl-30km and NoLZK and the corresponding wind difference (in dark contours) at the 36-h forecast time (1200 UTC 25 January 2000). The 36-h forecast differences have clearly developed more small-scale structure than that in the initial-difference field; associated with this small-scale structure, maximum wind and temperature (not shown) differences are

as large as 15 m s^{-1} and 5 K, respectively. Correspondingly, Fig. 15b shows there is a large-magnitude (40 mm) difference over the Atlantic Ocean in 36-h accumulated precipitation concentrated at small scales. (Even over North Carolina, the difference remains significant, as evidenced by the 11.2-mm maximum difference near Raleigh. Note also that these differences are not merely an overall shift in precipitation shield, but represent a rearrangement of the precipitation at smaller scales.) Power spectrum analysis of the difference between NoLZK and Cntl-30km at 0- and 36-h forecast time (Fig. 13a) verifies our subjective impression from Fig. 14a that the forecast differences at smaller scales grow and those at larger scales decay.

At first sight, one might suppose that the changes in precipitation produced by withholding the LZK sound-

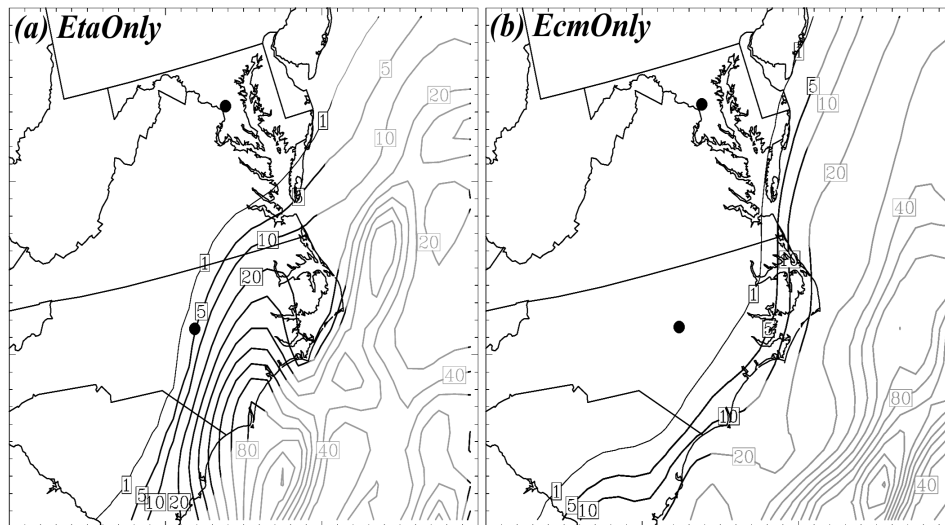


FIG. 12. As in Fig. 1(c) except for (a) EtaOnly, and (b) EcmOnly.

ing arise because that sounding lies in an area in which the initial conditions have a particularly strong influence on the precipitation forecast. (Areas of strong sensitivity to initial conditions are often identified by adjoint studies such as Rabier et al. 1995.) To test this possibility, we have performed other experiments in which soundings from other locations were withheld. These experiments will be referred to as NoAMA, NoTLH, etc., where the location of each sounding is given in Table 1; for experiment NoREV, soundings from both REV and BOI were withheld. Figure 14 shows the magnitude of 300-hPa wind differences in the initial conditions (gray contours) and in the 36-h forecast from four of these experiments.¹

Regardless of which sounding is withheld from the initial conditions, the 36-h forecast differences from Cntl-30km have qualitatively similar small-scale structure, and are concentrated in the same portion of the domain. The fact that even stations as far away from the Atlantic Ocean (where the difference fields in Fig. 14 are largest) as Reno, Nevada (REV), produce significant small-scale forecast differences, leads to the conclusion that there is a strong sensitivity to initial conditions in the small scales, which in turn suggests fundamental limitations on the predictability of those scales. As mentioned above, differences in the 36-h accumulated precipitation forecast with and without the LZK sounding are as large as 40 mm off the Atlantic

coast (Fig. 15a). Denial of other individual soundings had similar impacts on the precipitation forecasts. The total 36-h accumulated precipitation averaged over a $240 \text{ km} \times 240 \text{ km}$ grid box (shown in Fig. 15a) surrounding Raleigh can be altered by $\pm 40\%$ in all these individual sounding experiments (Fig. 15b). Even stronger variation of the averaged accumulated precipitation exists when averaged over a smaller domain, indicating the great uncertainty in the precipitation forecast at small scales. In summary, omitting even a single sounding from the initial conditions produces significant changes in the precipitation forecast, although mean sea level pressure is influenced only slightly. This strong sensitivity of precipitation forecast to small initial differences is consistent with rapid error growth of differences at smaller scales and suggests fundamental limitations of predictability of the mesoscale precipitation pattern within the large-scale system.

c. Discussion

The experiments described in the previous sections indicated that forecast differences grow rapidly at smaller scales while decaying considerably at larger scales. In this section, we will explore further the reasons for this scale dependence.

Given the association of the forecast differences with the regions of moist ascent and (parameterized) convection within the storm (e.g., Fig. 14), one might expect that the growth of small-scale differences is related to moist processes. To test this, fake-dry simulations were run in which the effects of latent heating were turned off in Cntl-30km and EtaOnly. Figure 13b shows the kinetic energy spectrum for the difference at 36 h between the two fake-dry simulations. Growth at the smaller scales is much reduced relative to that found in the corresponding moist simulations (cf. FD-Eta with

¹ The forecast differences at this time are close to the eastern boundary of the model domain. Since the boundary of the MM5 domain is limited by the use of the Eta 104-grid for initialization, it is not convenient to extend the boundary in these experiments. However, similar individual sounding experiments were performed using the ECMWF analysis with a much-extended MM5 domain. The results are very similar (not shown) and thus the concentration of forecast differences off the U.S. coast in Fig. 14 is not an artifact of the computational boundary conditions.

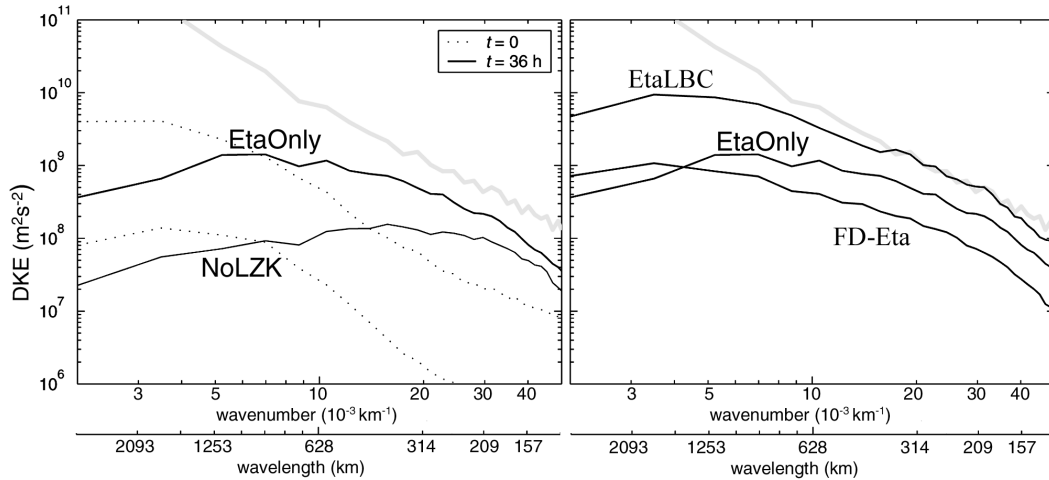


FIG. 13. Spectrum distribution of DKE between experiments. (a) Cntl-30km-EtaOnly and Cntl-30km-NoLZK at 0-h (dotted curves) and 36-h (solid curves) forecast; and (b) FD-30km-FD-Eta, Cntl-30km-EtaOnly, and EtaOnly-EtaLBC at 36-h forecast. Thick gray curves indicate spectrum analysis of the basic state kinetic energy averaged through the entire 36-h forecast period.

EtaOnly), thus confirming the importance of moist processes to such growth.

We now turn to the decay of forecast differences found at synoptic scales in Fig. 13. This decay stands in contrast to common experience in global models, where forecast differences grow substantially at syn-

optic scales (e.g., Simmons et al. 1995). Of course, it is also well known that synoptic-scale growth will be inhibited in the comparison of two limited-area simulations with identical lateral boundary conditions (Vukicevic and Errico 1990, and references therein).

To confirm the role of the lateral boundary conditions,

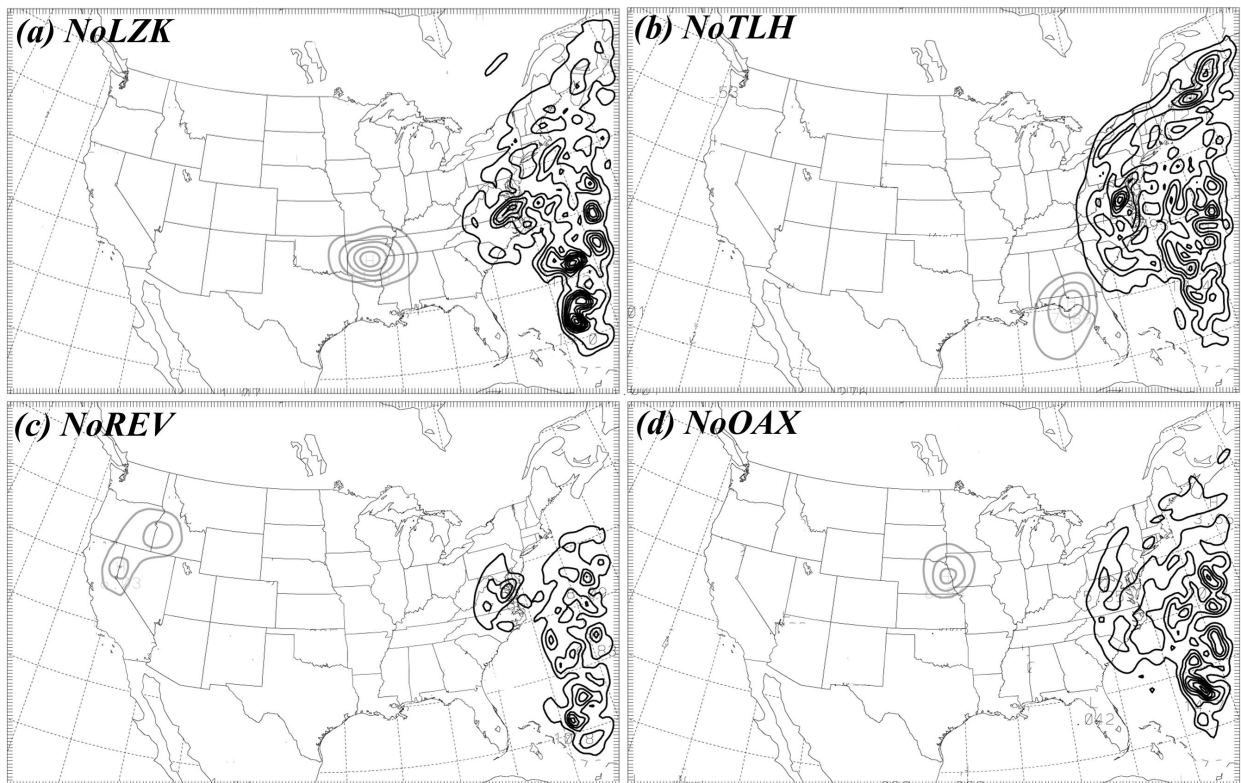


FIG. 14. The 300-hPa magnitude of wind difference (every 2 m s^{-1}) valid for 0-h (gray) and 36-h (dark) forecast between experiments Cntl-30km and (a) NoLZK, (b) NoTLH, (c) NoREV, and (d) NoOAX.

TABLE 1. List of the individual sounding locations.

Station		Location	State	Lat (°N)	Lon (°W)	Elev (m)
ID	No.					
AMA	72363	Amarillo	TX	35.22	101.70	1099
LZK	72340	Little Rock	AR	34.83	92.25	165
SIL	72233	Slidell	LA	30.25	89.77	3
ILN	72426	Wilmington	OH	39.42	83.72	317
REV	72489	Reno	NV	39.57	119.79	1515
OAX	72558	Valley	NE	41.32	96.37	350
ABQ	72365	Albuquerque	NM	35.04	106.60	1613
ALB	72518	Albany	NY	42.75	73.80	89
BOI	72681	Boise	ID	43.57	116.22	874
GSO	72317	Greensboro	NC	36.08	79.95	270
TLH	72214	Tallahassee	FL	30.40	84.35	18

a simulation (EtaLBC) was run as in EtaOnly except that the previous 12-h operational Eta forecast was used for the lateral boundary conditions. That is to say, MM5 in the EtaLBC simulation is initialized with the Eta analysis from 0000 UTC 24 January 2000 as in EtaOnly, but uses the tendency forecast from the Eta Model initialized at 1200 UTC 23 January as the lateral boundary condition. The kinetic energy spectrum for the difference between this simulation and EtaOnly at 36 h appears in Fig. 13b. As can be seen from Fig. 13b, the alterations to the boundary conditions produce significant growth at all the scales that decayed in EtaOnly. Further evidence of this “sweeping” of differences from the limited domain is provided by the growth of synoptic-scale differences in simulations (now initialized with ECMWF analysis) in which only initial conditions are perturbed but the domain is extended 1500 km to the east of the eastern boundary of the current D1 (not

shown). It thus seems reasonable to conclude that the decay of synoptic-scale differences found in Fig. 13 is an artifact of our limited-area simulations, and that differences at those scales would in fact grow, as has been found previously in global models.

The 300-hPa wind differences provide some sense of the relationship of the smaller-scale differences to those at synoptic scales. Figure 16 shows the 24-h differences between Cntl-30km and EtaOnly and between EtaLBC and EtaLBC. There is little difference between Cntl-30km and EtaOnly in the western two-thirds of the domain (Fig. 16a), whereas altering the boundary conditions fills that same portion of the domain with synoptic-scale differences (Fig. 16b). In the eastern one-third of the domain where there is moist ascent and parameterized convection, however, both fields display qualitatively similar small-scale structure, much as in our other simulations (Fig. 14). This indicates that the two sources of error growth (at different scales) are, to a first approximation, independent in these simulations.

In summary, these experiments suggest distinct mechanisms for error growth acting at synoptic scales and at mesoscales. The error growth at small scales is intimately related to the presence of moist processes in the flow, while the error growth at synoptic scales appears to be that familiar from predictability studies with global models. Except for Ehrendorfer et al. (1999) (discussed further in section 7), no other study using a limited-area model has identified such error growth at subsynoptic scales. In particular, Vukicevic and Errico (1990) perform broadly similar experiments and find that errors decay at subsynoptic scales. Our results may perhaps be reconciled with theirs by noting that their initial per-

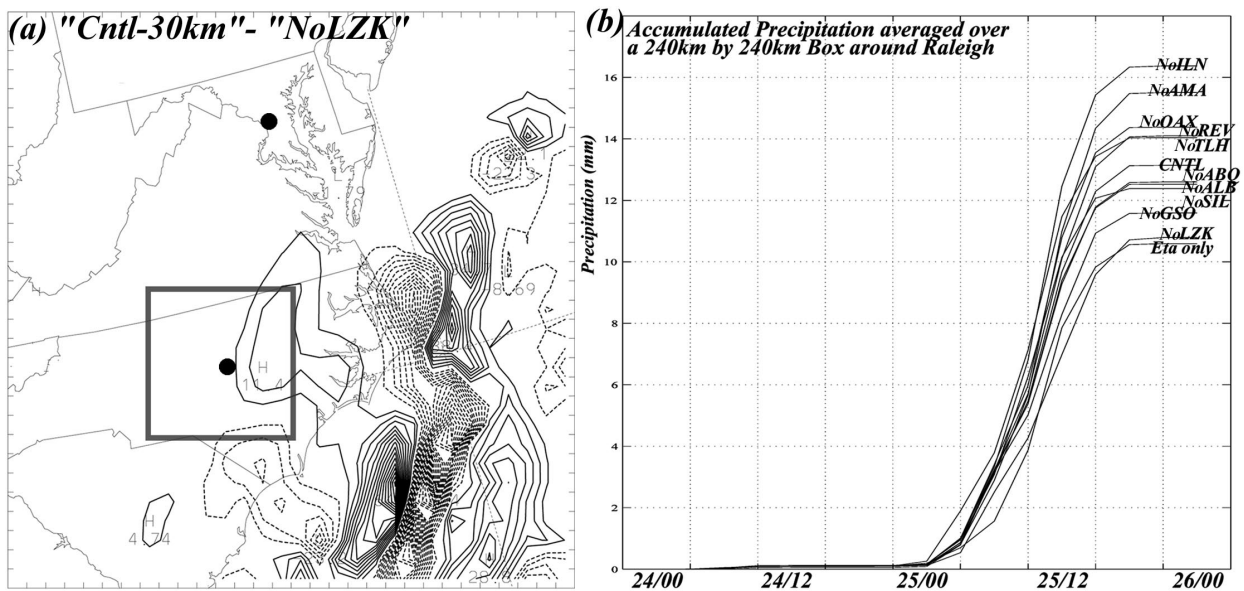


FIG. 15. (a) The 36-h accumulated precipitation difference (every 4 mm) between Cntl-30km and NoLZK. (b) Time evolution of the accumulated precipitation (mm) averaged over a 240-km × 240 km box around Raleigh, NC, from each individual sounding experiment, Cntl-30km and EtaOnly. The location of the box is shown in (a).

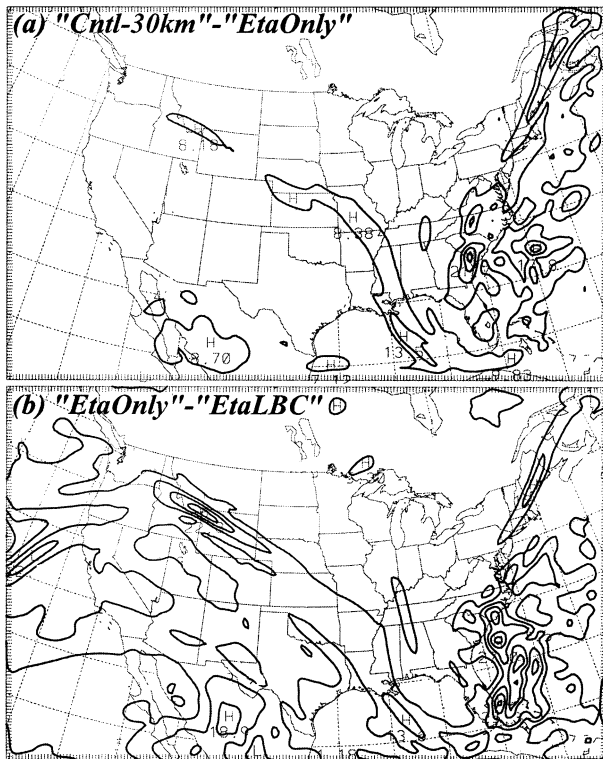


FIG. 16. The 300-hPa magnitude of wind difference (every 5 m s^{-1}) valid at 0000 UTC 25 Jan 2000 between EtaOnly and (a) Cntl-30km, (b) EtaLBC.

turbations were significantly larger than ours at the smaller scales and thus may have had no potential for growth prior to their saturation through nonlinearity. Also, these discrepancies may arise from the different synoptic situations studied, for example, the error growth in their simulation may have been less driven by moist processes.

Clearly, there is a need for further investigation of the small-scale growth found here. The outstanding issues include the precise role of moist processes, particularly moist convection, in the growth of small-scale errors, the possibility that the small-scale growth is an artifact of the physical parameterizations rather than a real property of the atmosphere, and the influence of the small-scale error growth on larger scales. These further issues will be investigated in a companion paper.

7. Summary and discussion

This study uses the Mesoscale Model MM5 to investigate possible sources of forecast error for the 24–25 January 2000 snowstorm along the east coast of the United States, concentrating on the quantitative precipitation forecast out to lead times of 36 h. Simulations were performed with various grid resolutions and initial conditions, and it was found that insufficient resolution and errors in the initial conditions both likely contrib-

uted significantly to problems in the forecast. Further experiments, in which individual soundings were withheld from the control analysis, show that the deficiencies in the initial conditions are unlikely to have arisen from poorly fitting one or two crucial soundings. The simulations with different initial conditions also have more general implications for the limits of predictability for the mesoscale precipitation distribution, as they exhibit rapid growth of forecast errors at scales below 600 km. Further expansion upon each of these topics follows.

Increased resolution alters the model's representation of moist processes resulting in the crucial changes to the simulation of upper-level features. Simulations without latent-heat release, in contrast, show little dependence on the resolution. These changes in the moist simulation, which accrue mainly in decreasing the grid spacing from 30 km to 10 km and less so from 10 km to 3.3 km, improve the forecast of the cyclone strength and location moderately, but result in notable improvements to the precipitation. This suggests that the planned increase in resolution of operational forecasts to O(10 km) will improve quantitative precipitation forecasts and subsequent increases in resolution will require further justification.

Aside from these simulations with different resolutions, the role of model error in this forecast has not been explicitly addressed, in part because of the difficulty of designing even marginally comprehensive and systematic experiments. Size of differences produced by changing resolution, however, indicates that model error is likely comparable to other sources of forecast error in this case. Other evidence supports this view. For example, changing the moist-convective parameterization from the Grell scheme to Betts–Miller results in an 8-hPa deepening of the surface cyclone (although using the Kain–Fritsch scheme produces little noticeable difference from the Grell scheme). In addition, the operational Eta forecast is arguably an outlier among the set of MM5 simulations from different analyses.

The dependence of the simulations on initial conditions was evaluated by initializing the model with a number of equally plausible analyses. The standard MM5 initialization, which used the operational Eta analysis as a first guess and adjusted the analysis toward the existing surface and upper-air observations, produced the best forecast, although the generality of this result is unclear. Use of these different analyses altered synoptic-scale aspects of the forecast, such as the cyclone position, by amounts comparable to the operational forecast error at similar lead times, and it is therefore concluded that errors in the initial conditions likely accounted for a substantial portion of the operational forecast errors.

As in the experiments with differing model resolution, the changes in the precipitation were again larger than changes in the strength or position of the surface cyclone. Consistent with this, forecast differences as measured by the domain-average total energy steadily in-

creased at scales below 600 km but, because lateral boundary conditions were not perturbed, decreased at larger scales.

Also considered was the possibility that the benefits of the MM5 initialization arose from better fitting one or a few key observations. In fact, the removal of any single sounding from the MM5 analysis produced only marginal changes in the forecast of cyclone strength and position. This is because the initial differences in these experiments were small and again decreased at synoptic scales as the forecast progressed. Forecast differences at scales below 600 km, however, grew even more rapidly than when their initial amplitude was larger, so that by 36 h they and the accompanying differences in the precipitation forecast were nearly as large as those produced by using different analyses.

The documentation of such rapid forecast-difference growth at scales below 600 km is an important result of this paper. The physical processes involved appear to be distinct from those familiar at synoptic scales (which, as discussed in section 6c, are inhibited here by fixed lateral boundary conditions). In particular, and as demonstrated by simulations without latent heating, the growth at small scales requires moist processes. The precise mechanisms for this rapid mesoscale error growth, however, are still uncertain. Moreover, much of the spectral range below 600 km is near the grid resolution in these simulations and is therefore subject to the uncertainties of both imperfect physical parameterization and numerical truncation errors. We defer to a companion paper all questions related to the growth mechanism or the roles of limited resolution and imperfect parameterizations.

Except for Ehrendorfer et al. (1999), other investigations have not found mesoscale error growth to be particularly rapid or to depend on moist processes. We believe such results arise from combinations of coarse resolution and initial perturbations that already have substantial amplitude at mesoscales. Our results complement those of Ehrendorfer et al., who calculated the leading singular vectors for a mesoscale model with moist physics by showing that even differences between plausible analyses will grow rapidly at the mesoscale. The precise relation of our results to those of Ehrendorfer et al. (1999) remains uncertain, as they employed adjoint techniques that depend on linearizations of the difference evolution, while we find (Fig. 13) that growth rates at small scales depend on the difference amplitude, suggesting that nonlinearity is important.

The results of this study also have broader implications for the forecasting and predictability of precipitation. First, they emphasize the difficulty of forecasting precipitation relative to, say, surface pressure. This problem may unfortunately be worse for precisely those forecasts in which precipitation is substantial, since the rapid small-scale error growth documented here depends on moist processes. In addition, the growth of small-scale differences clearly imposes an upper bound on the predict-

ability of the flow, much as foreseen by Lorenz (1969). In this specific case, our experiments withholding single soundings from the control analysis show that even small changes in the initial conditions may significantly alter the mesoscale distribution of precipitation within 24 or 36 h. This suggests that detailed precipitation forecasts for this event would be impossible beyond 2–3 days, even given greatly improved analyses. Thus, such limited predictability may of practical interest for numerical weather prediction even in the near term.

Acknowledgments. The authors are very grateful to both reviewers for their constructive comments for improving our manuscript and to Jim Bresch and Wei Wang for help in setting up the experiments and many helpful discussions. Thanks also go to Mel Shapiro, Chris Davis, Jimmy Duhdia, Morris Weisman, Craig Epifanio, Tom Hamill, Lance Bosart, Michael Kaplan, Steven Koch, David Muraki, and Kermit Keeter for their comments on the simulations. Davis and Epifanio also provided thorough and insightful reviews of an earlier version of this manuscript. This study is supported by U.S. Weather Research Program.

REFERENCES

- Anthes, R. A., Y. H. Kuo, and J. R. Gyakum, 1983: Numerical simulations of a case of explosive marine cyclogenesis. *Mon. Wea. Rev.*, **111**, 1172–1188.
- , —, D. P. Baumhefner, R. P. Errico, and T. W. Bettge, 1985: Predictability of mesoscale atmospheric motions. *Advances in Geophysics*, Vol. 28B, Academic Press, 159–202.
- Benjamin, S. O., and N. L. Seaman, 1985: A simple scheme for objective analysis in curved flow. *Mon. Wea. Rev.*, **113**, 1184–1198.
- Bosart, L. F., C. Lai, and E. Rogers, 1995: Incipient explosive marine cyclogenesis: Coastal development. *Tellus*, **47A**, 1–29.
- Davis, C. A., M. T. Stoelinga, and Y.-H. Kuo, 1993: The integrated effect of condensation in numerical simulations of extratropical cyclogenesis. *Mon. Wea. Rev.*, **121**, 2309–2330.
- Dickinson, M. J., L. F. Bosart, W. E. Bracken, G. J. Hakim, D. M. Schultz, M. A. Bedrick, and K. R. Tyle, 1997: The March 1993 superstorm cyclogenesis: Incipient phase synoptic- and convective-scale flow interaction and model performance. *Mon. Wea. Rev.*, **125**, 3041–3072.
- Duhdia, J., 1993: A nonhydrostatic version of the Penn State/NCAR Mesoscale Model: Validation tests and simulation of an Atlantic cyclone and cold front. *Mon. Wea. Rev.*, **121**, 1493–1513.
- Ehrendorfer, M., R. M. Errico, and K. D. Raeder, 1999: Singular-vector perturbation growth in a primitive equation model with moist physics. *J. Atmos. Sci.*, **56**, 1627–1648.
- Emanuel, K. A., 1985: Frontal circulations in the presence of small moist symmetric instability. *J. Atmos. Sci.*, **42**, 1062–1071.
- Errico, R., and D. Baumhefner, 1987: Predictability experiments using a high-resolution limited area model. *Mon. Wea. Rev.*, **115**, 488–504.
- Grell, G. A., 1993: Prognostic evaluation of assumptions used by cumulus parameterizations. *Mon. Wea. Rev.*, **121**, 5–31.
- Hou, Z., D. L. Zhang, and J. Gyakum, 1995: A diagnostic analysis of the superstorm of March 1993. *Mon. Wea. Rev.*, **123**, 1740–1761.
- Kocin, P. J., L. W. Uccellini, J. W. Zack, and M. L. Kaplan, 1985: A mesoscale numerical forecast of an intense snowburst along the East Coast. *Bull. Amer. Meteor. Soc.*, **66**, 1412–1424.
- Kuo, Y.-H., M. A. Shapiro, and E. G. Donall, 1991: The interaction

- between baroclinic and diabatic processes in a numerical simulation of a rapidly intensifying extratropical marine cyclone. *Mon. Wea. Rev.*, **119**, 368–384.
- , J. R. Gyakum, and Z. Guo, 1995: A case of rapid continental mesoscale cyclogenesis. Part I: Model sensitivity experiments. *Mon. Wea. Rev.*, **123**, 970–997.
- Lorenz, E. N., 1969: The predictability of a flow which possesses many scales of motion. *Tellus*, **21**, 289–307.
- Mellor, G. L., and T. Yamada, 1982: Development of a turbulence closure model for geophysical fluid problems. *Rev. Geophys. Space Phys.*, **20**, 851–875.
- Orlanski, I., and J. J. Katzfey, 1987: Sensitivity of model simulations for a coastal cyclone. *Mon. Wea. Rev.*, **115**, 2792–2821.
- Rabier, F., E. Klinker, P. Courtier, and A. Hollingsworth, 1995: Sensitivity of two-day forecast errors over the Northern Hemisphere to initial conditions. *Quart. J. Roy. Meteor. Soc.*, **121**, 121–150.
- Reisener, J., R. J. Rasmussen, and R. T. Bruintjes, 1998: Explicit forecasting of supercooled liquid water in winter storms using the MM5 Mesoscale Model. *Quart. J. Roy. Meteor. Soc.*, **124B**, 1071–1107.
- Simmons, A. J., R. Mureau, and T. Petroliagis, 1995: Error growth and estimates of predictability from the ECMWF forecasting system. *Quart. J. Roy. Meteor. Soc.*, **121**, 1739–1771.
- Uccellini, L. W., and Coauthors, 1995: Forecasting the 12–14 March 1993 superstorm. *Bull. Amer. Meteor. Soc.*, **76**, 183–199.
- Vukicevic, T., and R. M. Errico, 1990: The influence of artificial and physical factors upon predictability estimates using a complex limit-area model. *Mon. Wea. Rev.*, **118**, 1460–1482.
- Whitaker, J. S., and C. A. Davis, 1994: Cyclogenesis in a saturated environment. *J. Atmos. Sci.*, **51**, 889–907.
- Zhang, F., S. E. Koch, C. A. Davis, and M. L. Kaplan, 2001: Wavelet analysis and the governing dynamics of a large-amplitude gravity wave event along the East Coast of the United States. *Quart. J. Roy. Meteor. Soc.*, **127**, 2209–2245.